Mem. S.A.It. Vol. 75, 700

Memorie della

Post-AGB *s*-processed stars and theoretical interpretation

R. Gallino[1], E. Arnone[1], M. Pignatari[1] and O. Straniero[2]

[1] Dipartimento di Fisica Generale, Universitá di Torino, Via P. Giuria 1, 10125 Torino, Italy; e-mail: gallino@ph.unito.it, pignatar@ph.unito.it
[2] Osservatorio Astronomico di Collurania, via Mentore Maggini, 64100 Teramo, Italy

Abstract. Post-AGB stars show the *s*-process signature and the carbon enhancement typical of their parent AGB stars at the end of the TP-AGB phase. The less luminous protoplanetary nebulae not showing C nor *s*-enhancement are interpreted as descendants of AGB stars of $M < \sim 1.2\ M_{\odot}$, whose envelope mass was too low for the third dredge up to occur.

1. Introduction

Post-AGB stars are FG supergiant stars evolving off the tip of the AGB phase and evolving at constant luminosity towards the protoplanetary phase. Post-AGB stars showing IR excess and the 21 μm emission feature are C-rich. Table 1 reports the main *s*-process characteristics of 11 objects from the recent literature (Van Winckel and Reyniers 2000; Reyniers et al. 2004, Reddy et al. 1999; Zacs et al. 1995). The data of six post-AGB stars by Van Winckel and Reyniers (2000), updated by Reyniers et al. (2004), have been obtained with high-resolution spectra and high signal to noise. Two more post-AGB stars with high-quality spectra, IRAS06530 and IRAS08143, have been included; as reported in Table 1, their *s*-process characteristics are quite similar to IRAS05341 and to IRAS23304, respectively. The range of metallicity of the post-AGB stars elencated in Table 1 extends from [Fe/H] = −1 up to [Fe/H] = −0.3.

Send offprint requests to: R. Gallino
Correspondence to: Dipartimento di Fisica Generale, Via P. Giuria 1, 10125 Torino (Italy)

2. AGB nucleosynthesis predictions

Post-AGB stars may be classified in the same class as the intrinsic AGBs, that is stars showing in their photosphere the signature of fresh nucleosynthesis products, ^{12}C and s-elements, manifactured in the He intershell, the thin region comprised between the H shell and the He shell. At the quenching of a thermal instability (TP) in the He shell, the convective envelope penetrates in the top layers of the He intershell, mixing with the surface freshly nucleosynthesized material (third dredge up, TDU). Among the intrinsic AGB stars are the MS and S stars showing Tc (see Busso et al. 2001 and references therein), the SC stars (Abia and Wallerstein 1998), and the C(N) stars (Abia et al. 2002). During a third dredge up episode, penetration of a small amount of protons from the envelope into the top layers of the He intershell gives rise to the formation of a so-called ^{13}C pocket (see review by Busso, Gallino and Wasserburg 1999). Subsequently, at H reignition the reaction chain ^{12}C(p,γ)^{13}N(β^{+})^{13}C takes place, followed by the activation of the ^{13}C(α,n)^{16}O reaction in radiative conditions

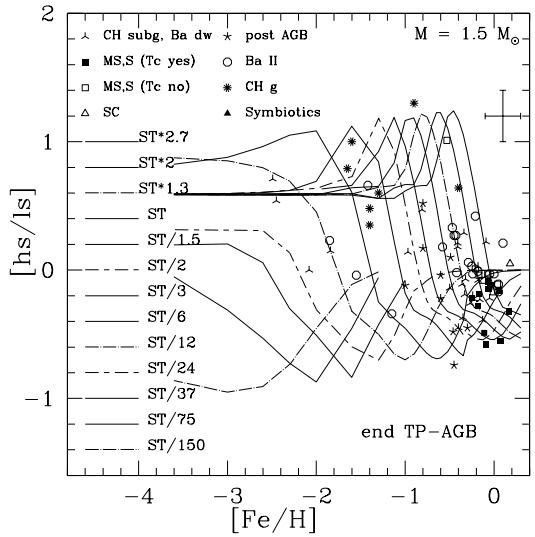

Fig. 1. Predicted trend of [hs/ls] versus [Fe/H] of stars of initial mass 1.5 $M_{\odot}$ at the end of the AGB phase as compared with spectroscopic observations of *s*-enhanced stars.

Table 1.

star	ref.	[Fe/H]	[ls/Fe]	[hs/Fe]	[hs/ls]	[s/Fe]
IRAS22223	(1)	−0.3	1.2	0.8	−0.4	0.9
IRASZ02229	(2)	−0.4	2.0	1.3	−0.7	1.5
IRAS07430	(2)	−0.5	2.1	1.6	−0.5	1.8
IRAS22272	(3)	−0.5	2.4	2.5	0.1	2.4
IRAS04296	(1)	−0.6	1.7	1.5	−0.2	1.5
IRAS19500	(1)	−0.7	1.4	1.0	−0.4	1.2
IRAS05341	(1)	−0.7	2.0	2.3	0.3	2.2
IRAS23304	(1)	−0.8	1.5	1.6	0.1	1.6
IRAS07134	(1)	−1.0	1.6	1.5	−0.1	1.5
IRAS06530	(4)	−0.5	1.8	2.2	0.4	2.1
IRAS08143	(4)	−0.4	1.5	1.5	0.0	1.5

References: (1) Van Winckel and Reyniers (2000), slightly updated by Reyniers et al. 2004; (2)Reddy et al. 1999; (3) Zacs et al. (1995); (4) Reyniers et al. 2004

in the interpulse period. At a given metallicity, a large range of ^{13}C-pocket efficiencies are required for the interpretation of the *s*-process distributions observed in *s*-enhanced stars (Busso et al. 2001). Stellar models predict at any metallicity wide ranges of [hs/Fe], [ls/Fe], [hs/ls], where ls=ls(Y, Zr) represents the first *s*-peak around neutron magic N = 50 and hs=hs(Ba, La, Nd, Sm) the second *s*-peak around neutron magic N = 82. Fig. 1 shows the predicted [hs/ls] versus [Fe/H] for AGB models of 1.5 $M_{\odot}$ and various ^{13}C pocket efficiencies at the end of the AGB phase. Mass loss was taken into account using the Reimers (1975) law with the η parameter set to 0.1. Very similar solutions are obtained using both a higher η and a higher initial mass, e.g. η = 0.3 and M = 2 $M_{\odot}$. The [hs/ls] is an intrinsic indicator, independent of the fact that the observed star is an intrinsic AGB or an extrinsic AGB. Extrinsic AGBs are main sequence or giant stars in close binary systems having been polluted by mass transfer from the more massive companion when it was on the AGB (now

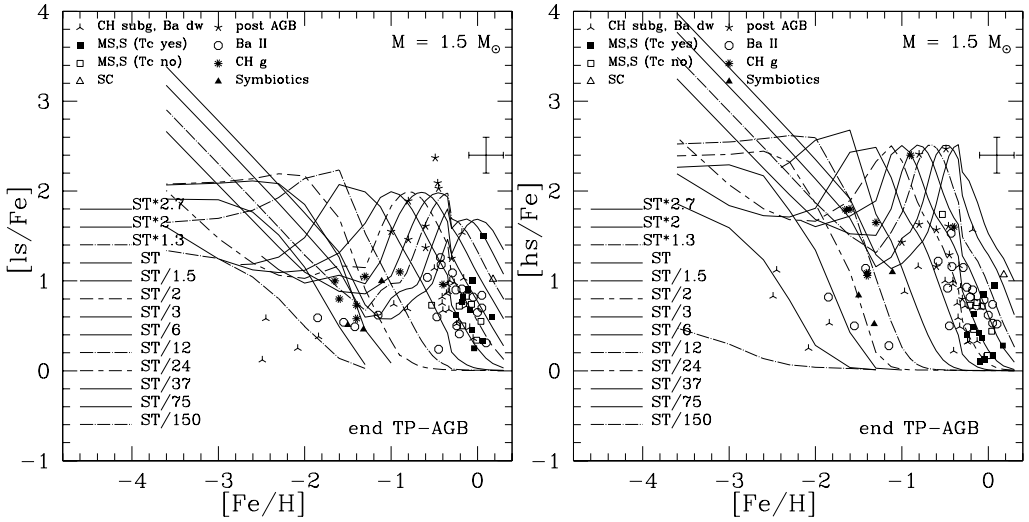

Fig. 2. *Left panel:* Predicted trend of [ls/Fe] versus [Fe/H] of stars of initial mass 1.5 $M_{\odot}$ at the end of the AGB phase as compared with spectroscopic observations of *s*-enanced stars. *Right panel:* The same for [hs/Fe].

a white dwarf). In Fig. 1, a collection of selected intrinsic and extrinsic AGBs is included for comparison (Arnone 2001). From Fig. 1 one sees that the post-AGB stars are well inside the general expectations of the *s*-enriched stars. Open problems are the observational link between binarity and post-AGB stars, and the evidence of dusty circumstellar disks around post-AGB stars with a likely segregation of carbon and heavy elements in the dust phase (Van Winckel 2003, see also these proceedings). In Fig. 1 only the six post-AGB stars revised by Reyniers et al. (2004) are reported. The spectra of IRASZ02229 and IRAS07430, and especially that of IRAS22272, are of lower quality. Among intrinsic AGBs, in Fig. 1 the MS and S stars showing Tc are included. The other intrinsic AGBs, the few SC stars (Abia and Wallerstein 1998) and the C(N) stars of about solar metallicity (Abia et al. 2001, 2002), have much more crowed spectra and a quite large uncertainty in their ls and hs abundance estimates.

A minimum mass of the envelope for which TDU takes place is predicted by our models, of ∼0.5 $M_{\odot}$. Consequently, we expect that the surface composition of the post-AGB stars be identical to that of the parent star at the tip of the AGB. This includes the regime of the so-called superwind (Iben and Renzini 1983). The AGB model predictions reported in Fig. 1 have been obtained for stars of initial mass 1.5 $M_{\odot}$ and η=0.1. The envelope *s*-process distribution varies in the first TPs followed by TDU, reaching an asymptotic distribution after about 10 TDU episodes. It may be interesting to examine what would happen for AGB models with less than 1.5 $M_{\odot}$ that develop a smaller number of TDU episodes. For them, the range of [hs/ls] expectations would shrink between a minimum [hs/ls] = −0.2 and a maximum [hs/ls] = +0.9. This means that stars with [hs/ls] < −0.2 should be considered of initial mass $M \geq 1.5\ M_{\odot}$ and in the late AGB phase. In Fig. 2 predictions of [ls/Fe] and [hs/Fe] versus [Fe/H] at the end of the AGB phase are compared with spectroscopic data. In the case of intrinsic AGB stars, the [ls/Fe] and [hs/Fe] ratios represent the surface composition, that is the mixture of material with original composition and *s*-rich material from the He intershell cumulatively mixed with the envelope by TDU episodes. For extrinsic AGBs, a further dilution is determined by the amount of AGB winds transferred and the envelope mass of the

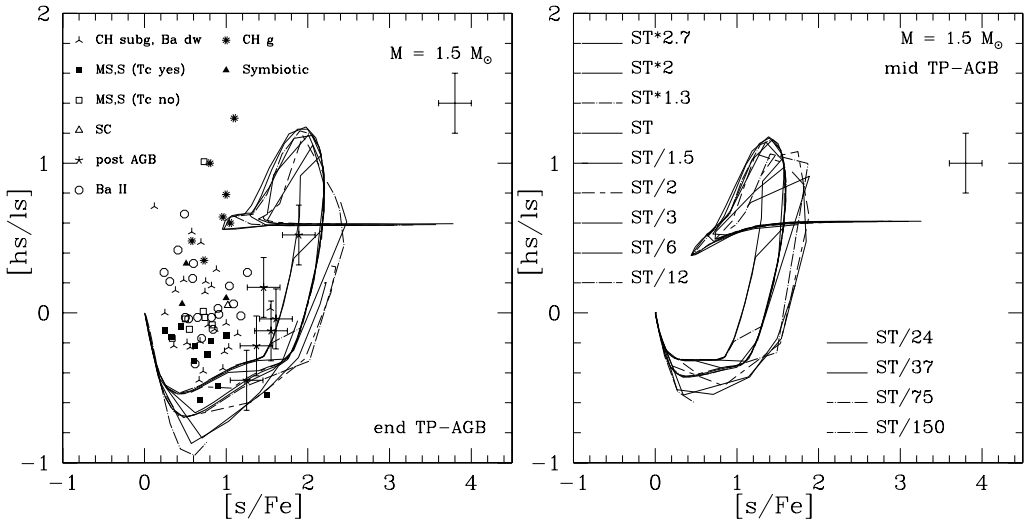

Fig. 3. Predicted trend of [hs/ls] versus [s/Fe] as compared with spectroscopic observations in the whole metallicity range shown in Fig. 1. Intrinsic AGBs are indicated with errorbars. The left panel is for AGB models of initial mass 1.5 $M_{\odot}$ at the end of the AGB phase, the right panel is for the envelope composition after the 8^{th} TDU episode, grossly equivalent to the final composition for AGB models of initial mass $\sim 1.3 M_{\odot}$.

secondary companion, the star now observed. The ^{13}C nuclei present in the pocket constitute a primary neutron source, while the *s*-process distribution depends on the number of neutrons captured by iron seed. Consequently, starting from [Fe/H] = 0, for a given choice of the ^{13}C pocket [ls/Fe] and [hs/Fe] first increase with decreasing the metallicity. The increase of [hs/Fe] is delayed at somewhat lower metallicity because of the bottleneck effect at the first *s*-peak around N = 50. The increase of [ls/Fe] reaches a maximum and then decreases, feeding the further increase of [hs/Fe]. At lower metallicities, also [hs/Fe] reaches a maximum and then decreases, when the second *s*-peak around N = 82 becomes saturated and the *s* fluence tends to accumulate at the termination of the s process, feeding the double magic nucleus ^{208}Pb (Z=82, N=126). As a consequence, the ratio [hs/ls] first increases with decreasing the metallicity, reaches a maximum and then decreases, driving the increase of the second intrinsic index, [Pb/hs] (Delaude et al. these proceedings). For lower ^{13}C pocket efficiencies, the entire behaviour is shifted at lower metallicities. A different way of comparing AGB predictions with spectroscopic observations is shown in Fig. 3, where the intrinsic index [hs/ls] is plotted versus [s/Fe], where [s/Fe] is the weighted average of [ls/Fe] and [hs/Fe]. Note that for any ^{13}C-pocket choice, the maximum in [hs/ls] is followed by a decrease in both [hs/ls] and [s/Fe] followed by an almost

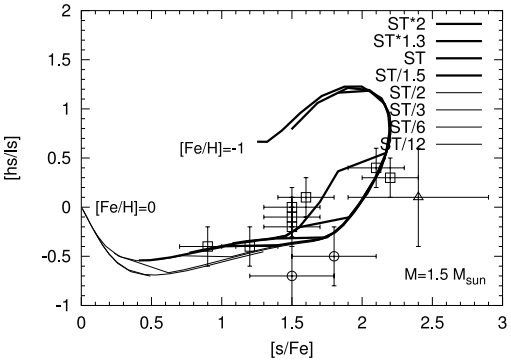

Fig. 4. Predicted AGB trend of the intrinsic index [hs/ls] versus [s/Fe] as compared with spectroscopic observations of post-AGB stars in the range of metallicities $-1 \leq$ [Fe/H] ≤ 0.

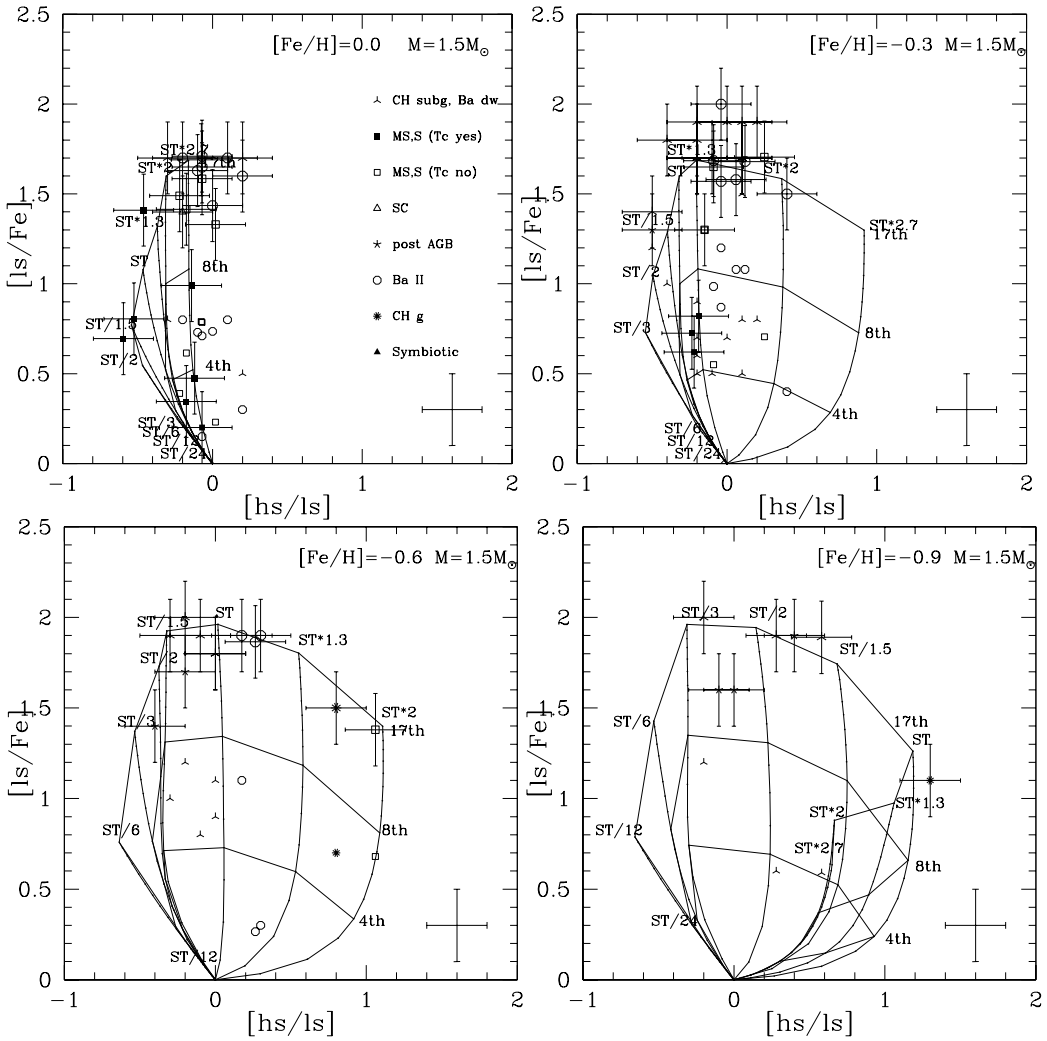

Fig. 5. Predicted [ls/Fe] versus [hs/ls] in the envelope of AGB stars of initial mass $M = 1.5 M_{\odot}$ and different ranges of metallicity compared with spectroscopic data of *s*-enhanced stars. Symbols with errorbars are intrinsic AGBs or parent stars of extrinsic AGBs. Lines connect results at the 4^{th}, 8^{th}, and at the end of the AGB.

flat curve with increasing [ls/fe] This upturn of the [hs/ls] trend versus [s/Fe] is caused by the progressive feeding of Pb by the *s* fluence. The spectroscopic data of six intrinsic post-AGB stars by Van Winckel and Reyniers (2000) are indicated with typical errobars, and the same is for the intrinsic MS and S stars. The left panel in Fig. 3 is for AGB model predictions of initial mass 1.5 $M_{\odot}$ at the end of the AGB phase, while the right panel is for the envelope composition after the 8^{th} TDU episode, grossly equivalent to the final composition for AGB models of initial mass around 1.3 $M_{\odot}$. One may recognize that all post-AGB stars are in the range of AGB predictions, with IRAS07134 and IRAS08143 being likely originated by a parent AGB star of around 1.3 $M_{\odot}$ (see discussion in Busso et al. 2001). Instead, only about half of MS and S stars agree with the

predicted trend, while the second group may be reconciled with expectations after a limited number of TDU episodes, as is shown in the left panel, where predictions after the 8^{th} TDU are shown. One should recall that intrinsic MS and S stars have not reached yet the tip of the AGB phase. The same is true for the C(N) stars (Abia et al. 2002). The observed C(N) stars show a C/O ratio very close to 1, after which the star becomes easily obscured by a very efficient formation of carbonaceous dust in the circumstellar envelope. All extrinsic AGB stars would shift to higher [ls/Fe] to represent their parent AGBs in the predicted region, once the dilution factor between the winds of the parent star and the envelope of the observed star is taken into account. This dilution factor is determined by the comparison of both observed [ls/Fe] and [hs/Fe] with theoretical expectations (Arnone 2001). A very interesting plot is shown in Fig. 4, where the [hs/ls] predictions versus [s/Fe] in the range of metallicity $-1 <$ [Fe/H] < 0 quite naturally explains the close-to-linear correlation observed by Reyniers et al. (2004). Note that the data of the two post-AGB stars by Reddy et al. (1999) may be better reconciled with a higher estimated [Fe/H] (see discussion in Reyniers et al. (2004) about IRAS06530 and the results obtained for the same star by Hrivnak and Reddy 2003). In the various panels of Fig. 5 we present the [ls/Fe] trends versus [hs/ls] in the envelope of AGB stars of initial mass $M = 1.5\ M_{\odot}$ subdivided in four different ranges of metallicity and compared with observations. This diagram was suggested by Smith and Lambert (1990) for stars of composite metallicity. It combines the efficiency of mixing and the *s*-process elemental distribution. Note that the extrinsic AGB stars are reported twice, the first time as they are really observed, the second time as their parent AGB stars (symbols with errorbars) once a bestfit dilution factor is deduced from comparison of [ls/Fe] and [hs/Fe] data with AGB model predictions. Finally, according to our models, AGB stars with initial mass below the limit for the TDU to take place, $M \leq 1.2\ M_{\odot}$, will become post-AGB stars without showing any C- or *s*−enhancement. This minimum mass would somewhat increase with increasing the η Reimers' parameter. The existence of a limiting initial mass beyond which the third dredge up may occur explains the important fraction of O-rich post-AGB stars observed with no *s*-enrichment (Van Winckel 2003), as well as the dichotomy with the post-AGB discussed here, all of them showing an important *s*-enrichement.

Acknowledgements. Work partly supported by the Italian MIUR-FIRB Project Astrophysical Origin of the Heavy Elements beyond Iron.

References

Abia, C., et al. 2001, ApJ, 559, 1117
Abia, C., et al. 2002, ApJ, 579, 817
Abia, C., Wallerstein, G. 1998, MNRAS, 293, 89
Arnone, E., Universitá degli Studi di Torino, Degree in Physics, Thesis, 2001 (unpublished)
Busso, M., Gallino, R., Wasserburg, G.J., 1999, ARA&A, 37, 239
Busso, M., et al. 2001, ApJ, 557, 802
Hrivnak, B.J., Reddy, B.E. 2003, ApJ, 590, 1049
Iben, I.J., Renzini, A. 1983, ARA&A 21, 271
Reddy, B.E., Bakker, E.J., Hrivnak, B.J. 1999, ApJ 524, 831
Reimers, D. 1975, in Problems in Stellar Atmospheres and Envelopes, eds. B. Bashek, H. Kegel, G. Traving, (New York: Springer-Verlag), 229
Reyniers, M., Van Winckel, H., Gallino, R., Straniero, O. 2004, A&A, 417, 269
Smith, V.V., Lambert, D.L. 1990, ApJS, 72, 387
Van Winckel, H. 2003, ARA&A, 41, 391
Van Winckel, H., Reyniers, M. 2000, A&A, 354, 135
Zacs, L., Klochkova, V.G., Panchuck, V.E. 1995, MNRAS, 275, 764